parallel to the plane of incidence ($\varphi = 45^\circ$), t_{s1}^0 vanishes, a result that is related to the polarizations of the fields.

IV. Conclusion

A formulation of the Rayleigh method for calculating the electromagnetic fields scattered by a periodically corrugated interface between an isotropic material and a gyroelectromagnetic uniaxial medium has been presented. The present method can handle general configurations in which the incident beam is associated to waves coming either from the isotropic or from the gyroelectromagnetic side and any orientations with respect to the grooves of the grating for the plane of incidence and for the optical axis of the anisotropic medium. Perfect agreement between the numerical results obtained with this formalism and previous results has been observed for for perfectly flat ($h/d \to 0$) gyroelectromagnetic interfaces and for corrugated gratings in classical mountings with the optic axis of the anisotropic material in the plane of the interface. Results for sinusoidal gratings with different values of h/d in classical and conical mountings were presented.

References

[1] R. E. Collin, *Foundations for Microwave Engineering*, 2nd ed. New York/Piscataway, NJ: Wiley-IEEE Press, 2000.

[2] J. Singh and K. Thyagarajan, "Analysis of metal clad uniaxial waveguides," *Opt. Communications*, vol. 85, pp. 397–402, 1991.

[3] A. Toscano and L. Vegni, "Spectral electromagnetic modeling of a planar integrated structure with a general grounded anisotropic slab," *IEEE Trans. Antennas Propag.*, vol. 41, pp. 362–370, 1993.

[4] L. Li, "Oblique-coordinate-system-based Chandezon method for modeling one-dimensionally periodic, multilayer, inhomogeneous, anisotropic gratings," *J. Opt. Soc. Amer. A*, vol. 16, pp. 2521–2531, 1999.

[5] A. Lakhtakia, R. Depine, M. Inchaussandague, and V. Brudny, "Scattering by a periodically corrugated interface between free space and a gyroelectromagnetic uniaxial medium," *Appl. Opt.*, vol. 32, pp. 2765–2772, 1993.

[6] M. E. Inchaussandague, M. L. Gigli, and R. A. Depine, "Reflection characteristics of a PML with a shallow corrugation," *IEEE Trans. Microw. Theory Techn.*, vol. 51, no. 1691, 2003.

[7] R. Petit, *Electromagnetic Theory of Gratings*, R. Petit, Ed. Heidelberg, Germany: Springer, 1980.

[8] R. Petit, "Plane wave expansions used to describe the field diffracted by a grating," *J. Opt. Soc. Amer.*, vol. 71, pp. 593–598, 1981.

[9] R. A. Depine and M. L. Gigli, "Diffraction from corrugated gratings made with uniaxial crystals: Rayleigh methods," *J. Mod. Opt.*, vol. 41, pp. 695–715, 1994.

[10] R. A. Depine and M. L. Gigli, "Conversion between polarization states at the sinusoidal boundary of a uniaxial crystal," *Phys. Rev. B, Condens. Matter*, vol. 49, pp. 8437–8445, 1994.

[11] H. C. Chen, *Theory of Electromagnetic Waves: A Coordinate Free Approach*. New York: McGraw-Hill, 1983.

[12] M. C. Simon and D. C. Farías, "Reflection and refraction in uniaxial crystals with dielectric and magnetic anisotropy," *J. Mod. Opt.*, vol. 41, pp. 413–429, 1994.

Negative Group Velocity and Anomalous Transmission in a One-Dimensionally Periodic Waveguide

Ruey Bing Hwang

***Abstract*—This study presents a theoretical investigation of the negative group velocity (NGV) and anomalous transmittance of waves in the stop band of a corrugated parallel-plate waveguide (CPPWG). The two different schemes, scattering analysis for a finite CPPWG and the dispersion relation of an infinite CPPWG, were used to investigate the physical insight of the wave process. The NGV zone corresponds to the stopband slanted at an angle on the Brillouin diagram, following the mutual verification of the results obtained by the two different approaches. This class of stopband is caused by the contra-flow interaction between the fundamental mode and the space harmonics of higher-order modes. Additionally, fluctuation was also found in the transmitted coefficient within the conventional stopband, caused by the excitation of the first higher-order mode within the stopband of the fundamental mode.**

***Index Terms*—Corrugated waveguide, negative group velocity, periodic structures.**

I. Introduction

The superluminal group velocity (that is, faster than the speed of light, c, in vacuum) and negative group velocities (NGVs) of the waves in an anomalous dispersion medium have previously been theoretically and experimentally studied [1]–[5]. Recently, Siddiqui, Mojahedi and Eleftheriades [6] designed a new artificial medium having both the Negative Refractive Index and the NGV properties. In their proposed framework, a resonant circuit is embedded within each loaded transmission line unit cell, generating an anomalous dispersion zone with a negative group delay [6]. Besides, dispersion analysis of Sievenpiper's shielded structure using multi-conductor transmission-line theory was carried out and the formation of a *slanted* stopband formed due to contra-directional coupling between the fundamental backward-wave harmonic and the underlying parallel-plate mode was found [7].

In this paper, the NGVs property of the waves guided in a corrugated parallel-plate waveguide (CPPWG) was investigated. The structure under consideration is a parallel-plate waveguide with periodic variation (corrugation) on its bottom wall. Such a CPPWG structure has been widely studied with its guiding characteristics in the pass- and stopbands regions [8]–[12], and has also been employed to design a surface-wave antenna [13]. Here, we took this structure as an example to examine its NGVs property, because that the structure is simple and the mathematical formulation is straightforward. Significantly, dispersion relation of the source-free fields supported by the CPPWG of infinite extent can be exactly predicted.

A rigorous mode-matching method was applied to study such a electromagnetic boundary-values problem consisting of multiple discontinuities. The input-output relation for each discontinuity was first formulated and expressed in terms of the generalized scattering matrix [14]. The scattering characteristics of the overall structure could be obtained by cascading the respective scattering matrix. Besides, the dispersion relation of the infinite periodic structure can be obtained by imposing the Bloch (periodic boundary) condition at the input and output interfaces of a unit cell. The dispersion relation was further converted

Manuscript received April 27, 2005; revised September 9, 2005. This research was supported by National Science Council, Taiwan, R.O.C., under the Contract NSC 94-2213-E-009-069.

The author is with the Department of Communication Engineering National Chiao Tung University, Hsinchu, Taiwan, R.O.C. (e-mail: raybeam@mail.nctu.edu.tw).

Digital Object Identifier 10.1109/TAP.2005.863157

into an eigenvalue problem, where the eigenvalue denotes its dispersion root and the associated eigenvector stands for the mode field pattern.

From the previous literature [15]–[17], we know that scattering characteristics of plane waves by a finite periodic structure, however, with sufficiently large number of unit cells, can be well predicted from the dispersion relation of waves supported by the corresponding structure of infinite extent. Therefore, we employed two schemes to examine the NGV properties of this waveguide, the scattering analysis of a finite length CPPWG, and the dispersion relation of waves guided in the infinite CPPWG. The former allows us to know the transmitted and reflected responses, especially on its pass- and stop- bands behavior. Specifically, the phase and group velocities were obtained by processing the transmitted phase angle. The latter one can tell us the dispersion relation of the source-free (or resonance) fields supported by the infinite corrugated waveguide. In general, the dispersion roots are complex number, with their real- and imaginary- parts representing the phase- and attenuation- constants. To clearly observe the band structure, we drew the dispersion relation in terms of the format of the Brillouin diagram (the relationship between $k_o d/2\pi$ and $\beta d/2\pi$). The stop band caused by the contra-flow coupling between two space harmonics was also carefully identified by comparing exact dispersion relation with that of unperturbed one. By mutually verifying the property of NGV through the transmitted response and the dispersion characteristics of the corrugated waveguide, we found that it occurs in the stop-band region slanted at an angle on the Brillouin diagram, resulted from a contra-flow interaction between the fundamental mode and the space harmonics of higher-order waveguide modes.

This investigation is structured as follows. Section II introduces the structure of the corrugated parallel-plate waveguide. Section III outlines the mathematical procedure for the two problems, the scattering analysis of the finite length corrugated waveguide and the dispersion relation of the corresponding waveguide of infinite extent. Section IV presents the numerical results of negative group velocity obtained from scattering analysis. The NGV property was explained by the dispersion relation of an infinite corrugated waveguide. The conclusion highlights key features of the numerical experiment in this study.

II. Description of This Problem

Fig. 1(a) displays the structure of a metallic CPPWG. The structure typically is a parallel-plate waveguide with corrugated wall on its bottom surface. It contains two uniform sections of parallel-plate waveguides at its input and output ends, and corrugations otherwise. The structure infinitely extends along the y direction. The period is d along the z-axis. Fig. 1(b) shows a magnified unit cell of the periodic structure. Each unit cell includes two back-to-back step junctions. The channel width and the corrugation thickness are denoted by s and t, respectively. The slot width between two adjacent corrugations is designated as w. The medium filled inside the waveguide is set to be air. This work assumed that the structure and field did not vary along the y direction ($\partial/\partial y = 0$). Therefore, the problem can be considered as a scalar boundary-value problem in respective TE and TM polarization. Additionally, the incident wave is the fundamental mode of the uniform parallel-plate waveguide.

III. Method of Analysis

Previous literature [7], [9], [12] has derived the detailed mathematical formulation concerning the wave propagation in a CPPWG. Therefore, the procedures are outlined for reference. As depicted in Fig. 1(a), the CPPWG can be considered as the cascades of unit cells, each containing two step junctions. Firstly, we expand the tangential electric- and magnetic-fields in terms of the superposition of the PPWG modes in respective uniform PPWG region. Secondly, due to the electromagnetic boundary condition, the tangential components of the electric- and magnetic- fields have to be continuous across the step junction, resulting in the input-output relation of the step junction. Thirdly, by cascading the two input-output relations of the step junctions, the input-output relation of the unit cell could be obtained. Finally, the scattering characteristics could be further determined by successively cascading each unit cell. On the other hand, the dispersion characteristics of the source-free fields were obtained by imposing the Bloch (Floquet) condition on the unit cell.

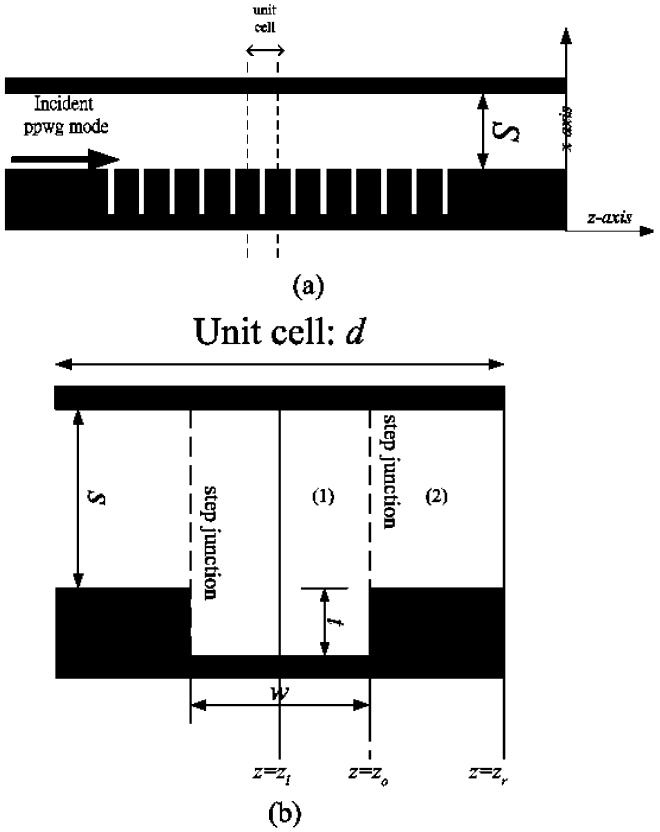

Fig. 1. (a) Structure configuration of a parallel-plate waveguide having periodic variation on its wall and (b) unit cell of the periodic waveguide.

A. Scattering Analysis for Finite Number of Periods

We assume that the CPPWG comprises N unit cells. After determining the input-output relation of the overall structure, the transmittance and reflectance for each mode can then be fully specified if the incident waves is given. As a consequence, the transmittance of the PPWG fundamental mode is written as: $V_t^{(n=0)} = V_o \angle\phi$, where ϕ represents the phase angle in radians and V_o is its amplitude. If the edge effect at the input and output ends are negligible (with sufficiently large number of unit cells), then the phase velocity could be approximated as $\phi \approx -\beta_{\text{eff}} L$, where L denotes total length of the CPPWG and β_{eff} represents the approximate phase constant of the periodic wave in the structure. Furthermore, the group index, defined as the ratio of c (speed of light in vacuum) to the group velocity, can be approximated as

$$n_g = C/v_g \approx -\frac{1}{L}\frac{d\phi}{dk_o}. \tag{1}$$

B. Dispersion Relation of the CPPWG of Infinite Extent

The voltage and current waves propagating through a unit cell experience a phase shift (Bloch condition), if the periodic structure is infinite in extent. The phase shift equals to $\exp(-j k_z d)$, where k_z is the propagation constant of the periodic wave along the z direction. This leads to

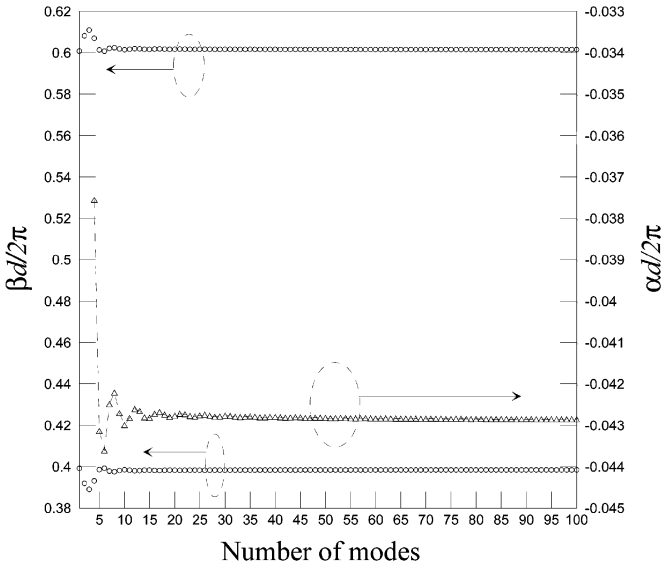

Fig. 2. Variation of the propagation constant against the normalized frequency; the lines marked with circles are normalized phase constant, while the line marked with triangles is normalized attenuation constant.

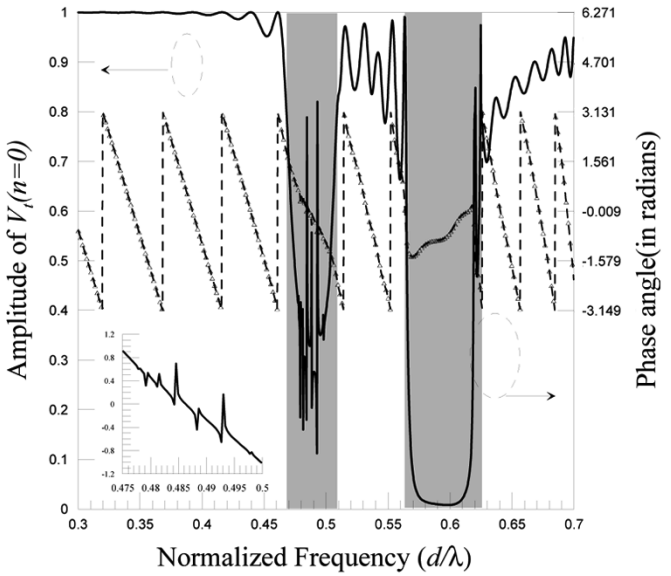

Fig. 3. Variation of $V_t(n = 0)$ against normalized frequency; the solid line represents the amplitude of transmittance, while the dash line marked with triangles is the phase angle in radians.

the dispersion relation of the CPPWG. The next procedure is to search the dispersion root k_z for a given frequency and structure parameters. The eigenvalues to the dispersion equation, in general, are complex numbers, with their real and imaginary parts denoting the phase and attenuation constants, respectively.

IV. Numerical Result and Discussion

Based on the previously defined equations, two computer programs were developed in this study, one for the dispersion relation of an infinite CPPWG and the other for the scattering analysis of a finite length CPPWG. Hereafter, we normalize all the structure parameters to the period d. The structure and incident parameters for the following examples are: PPWG channel width $s = 1.0d$, and slot width (w) and thickness (t) of corrugation were set to $0.1d$ and $0.28d$, respectively. The number of unit cells was set to $N = 20$. The incident waveguide mode was designated as the fundamental mode with TM polarization.

Before performing extensive numerical computations on the scattering and guiding characteristics, we first carry out the convergence test for the solution against the number of modes employed. Fig. 2 illustrates the variation of the z direction propagation constant $(k_z = \beta - j\alpha)$, including phase and attenuation constants, against the number of employed modes. In this case, to examine the capability for complex root searching, the normalized frequency was chosen as $d/\lambda = 0.6$, to obtain a complex root located inside a stopband. The line marked with circle denotes the real part of the dispersion root, while the one with triangle was that of the imaginary part. Here, the two complex roots share the same absolute value of the imaginary part, such that only one value was shown in this figure. The number of modes was progressively increased from 3 to 100 to examine the variation of roots for both the real- and the imaginary- parts. The dispersion roots appear to converge very well when the number of modes exceeds 20.

To investigate the NGV property associated with the CPPWG, a scattering analysis was performed, with the incident power of the PPWG mode (TM_o) set to unity. Fig. 3 display the variation of transmittance (fundamental mode voltage), including the magnitude and phase angle in radians, against the normalized frequencies (d/λ). The solid line represents the strength of the transmittance corresponding to the left-hand side axis, while the dashed line with triangles is the phase angle corresponding to right-hand side axis. The zones drawn in a shadow pattern demonstrate strong reflections for the incident wave. These two areas are stop bands owing to the in-phase reflection (Bragg reflection) from each discontinuity. However, it is interesting to note that some narrow pass bands appeared in the first stop band. Besides, the phase angle also exhibits rapid variations in this region. To facilitate observation, the phase angle distribution in the first stop band was enlarged and again plotted in the inset. This anomalous band structure has not been reported previously. This interesting phenomenon will be interpreted using the waveguide dispersion relation later.

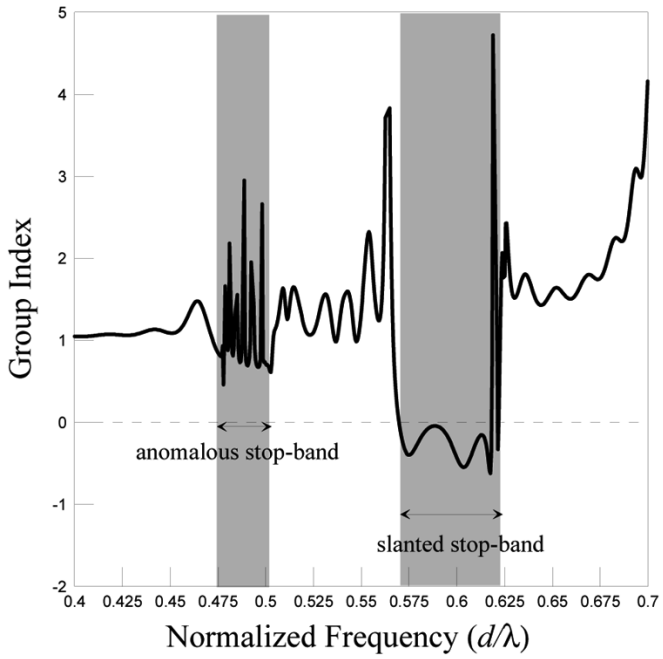

Fig. 4. Variation of group index against normalized frequency.

Fig. 4 depicted the variation of group index, computed by (1), against the normalized frequency (d/λ). The two stopband zones are highlighted in a shadow pattern. The right-hand side stopband, unlike the left-hand stopband, exhibits negative group index (or NGV). Recalling

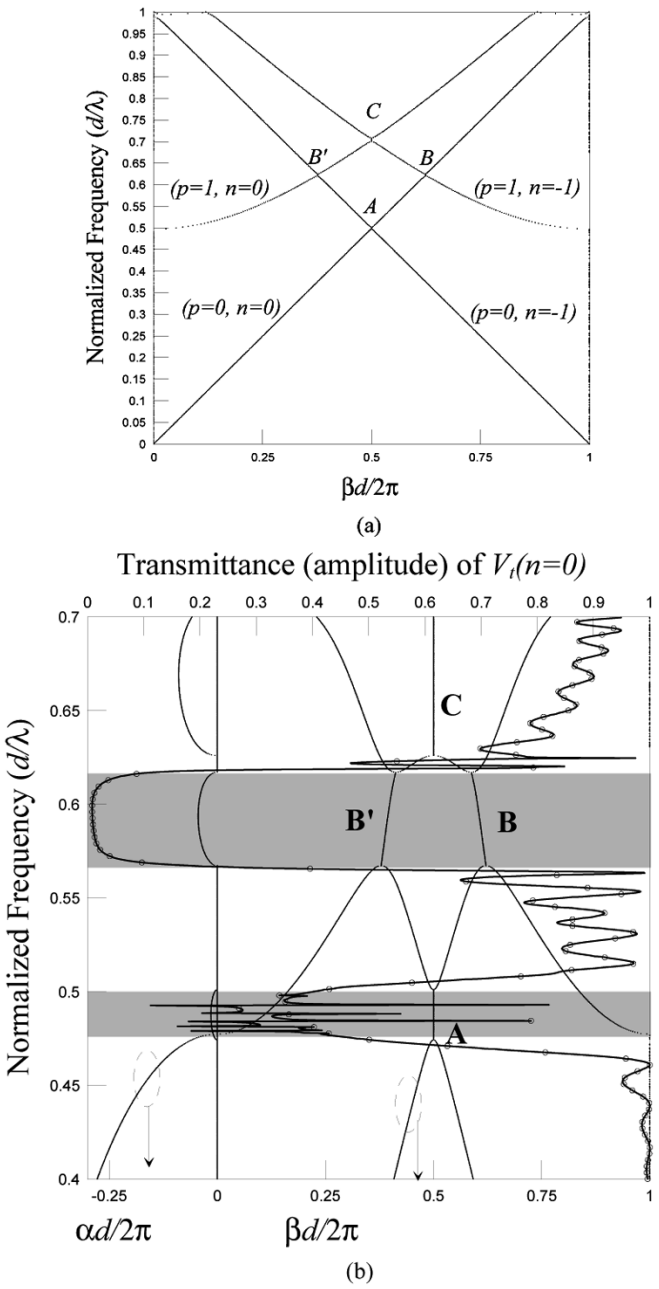

Fig. 5. Band structure of the periodic waveguide of infinite extent plotted in the format of Brillouin diagram: (a) Unperturbed dispersion curves and (b) exact dispersion curves obtained by generalized eigenvalue equation.

the phase angle distribution shown in Fig. 3, the slope of the phase angle is typically negative with respect to the frequency, excluding some fluctuations, but is positive in the second stopband region. Equation (1) reveals that the group index is proportional to the negative sign of the slope, which explains mathematically why the second stopband has a negative group index (NGV). However, what is the physical insight of wave propagation with NGV in the second stopband? To answer this question, the dispersion characteristics of the source-free fields supported by this CPPWG must be further investigated to understand the wave processes involved in such a stopband region.

To obtain a basic understanding of the wave-guiding phenomena in such a periodic waveguide, the unperturbed dispersion relation in the limiting case, when the thickness of the corrugation tends to zero, was plotted in Fig. 5(a). This plot helps us to know the possible physical effects, such as the phenomenon of mode coupling among the space harmonics, in the periodic waveguide. Fig. 5(a) illustrates the unperturbed dispersion curves, where the vertical axis represents the normalized frequency d/λ, while the horizontal axis is the propagation constant along the z direction. Each curve corresponds to the space harmonic with the index pair (p, n), where p denotes the pth mode supported by the waveguide, and n represents its corresponding space harmonic. Moreover, the set of straight lines, given by (0, 0) and $(0, -1)$, belongs to the fundamental mode of the waveguide, while the other set of hyperbolic curves corresponds to the first higher-order mode of the waveguide. From the coupled-mode theory, the phase matching condition takes place at the intersection point among the dispersion curves, possibly leading to a contra-flow or co-flow interaction. A contra-flow interaction causes a stop band where the wave experiences strong attenuation. The intersection points are labeled in alphabetical order, and help explain the phenomena of NGV, as explained later.

Fig. 5(b) depicted the exact dispersion relation displayed in terms of the Brillouin diagram. The vertical axis represents the normalized frequency d/λ, while the horizontal one denotes the propagation constant, including the phase $\beta d/2\pi$ (right-hand side) and attenuation $\alpha d/2\pi$ (left-hand side) constants. Additionally, the distribution of transmittance versus normalized frequency is also plotted (line with circles) in this figure for easy reference.

Comparing Fig. 5(b) with (a), the actual dispersion curves appear to follow the unperturbed curves. The strong contra-flow interactions (or coupling) arise around the interaction points labeled by A, B, B' and C. The stopband given by B and B' is *slanted* at an angle on the Brillouin diagram, which distinguishes it from the conventional stop bands A and C. Recalling the unperturbed dispersion curves in Fig. 5(a), it is recognized that the slanted stop band was results from the interaction between the fundamental and the space harmonic of the first higher-order modes. Since the dispersion curve corresponding to the transmitted wave follows the path through region A and B, the slope of the dispersion curve within the stop band B is negative with respect to the attached axes. It means that the $d\beta/dk_o$ is negative, causing a negative group index. Additionally, the first-higher order mode apparently exhibits pure imaginary dispersion roots (below cutoff), when the normalized frequency is below $d/\lambda = 0.478$.

The first stopband between $d/\lambda = 0.46$ and $d/\lambda = 0.5$ consists of some fluctuations, as previously mentioned. The first spike (pass band) shown in Fig. 5(b) occurs at $d/\lambda = 0.478$, corresponding to the cutoff normalized-frequency of the first higher-order PPWG mode, as illustrated in this figure. The stopband inhibited the propagation of fundamental mode and its space harmonic, as demonstrated from the dispersion curves. However, the first higher-order mode began to propagate at the frequency within the stop band. The coexistence of the stop band and the above-cutoff first higher-order mode caused the transmittance response to fluctuate.

Fig. 6 illustrates the variation of group index versus normalized frequency for various lengths of CPPWG (or number of unit cells). The amount of the group index is closely related to the length of the periodic waveguide, indicating that the increase in the length of the CPPWG generally increases the group delay, as confirmed by intuition.

The anomalous transmittance occurs when the excitation of first higher-order mode falls within the stopband region, as was demonstrated in the previous numerical example. To prove that the coexistence of the stop band and the propagating higher-order mode may cause transmittance fluctuations, the separation distance $(s = 0.8d)$ and the thickness of corrugation $(t = 0.25d)$ were changed to shift the cutoff frequency out of the stopband region. Fig. 7 illustrates the distribution of phase constant and group index against the normalized frequency of the finite length CPPWG. The dispersion relation of the corresponding infinite CPPWG is also computed and plotted in the same figure for easy comparison. Significantly, the fluctuation in

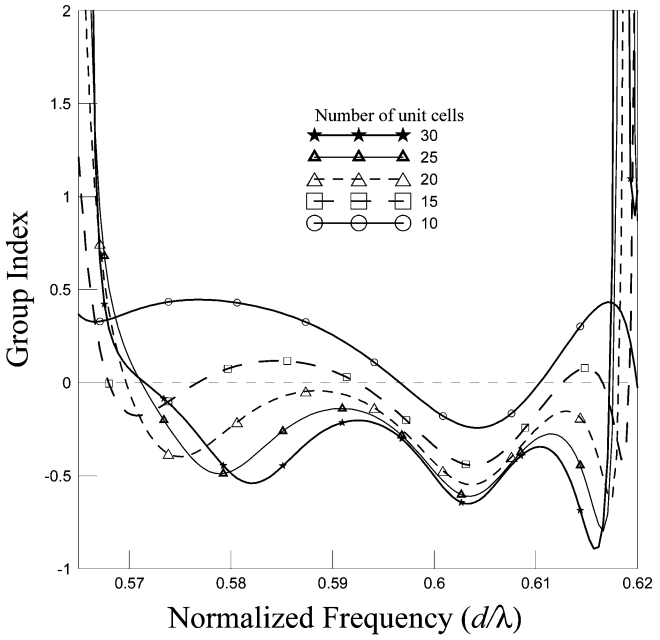

Fig. 6. Variation of group index against normalized frequency for various waveguide lengths.

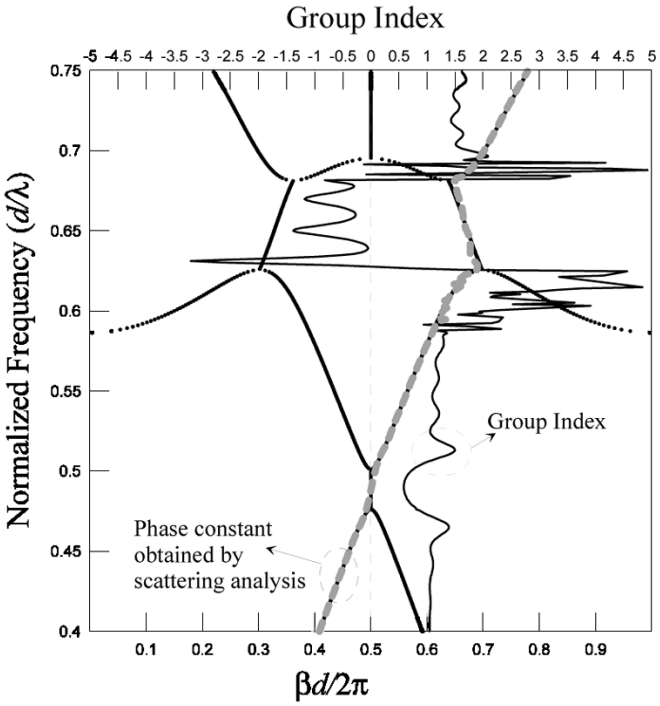

Fig. 7. Distribution of phase and group index against the normalized frequency of the finite length CPPWG; the line in gray color represents the phase constant evaluated by the phase response of transmittance.

the transmittance *disappears*, since the cutoff frequency of the first higher-order mode was not in the first stopband region. That is, no higher-order propagation modes were excited within the frequency range of the stopband. Therefore, the transmittance response has a pure attenuation in the stopband region. Additionally, the distributions of phase constants obtained by scattering analysis (in dash line with gray color) and dispersion relation analysis have a similar variation, which again validates the correlation between the NGV and the slanted stopband.

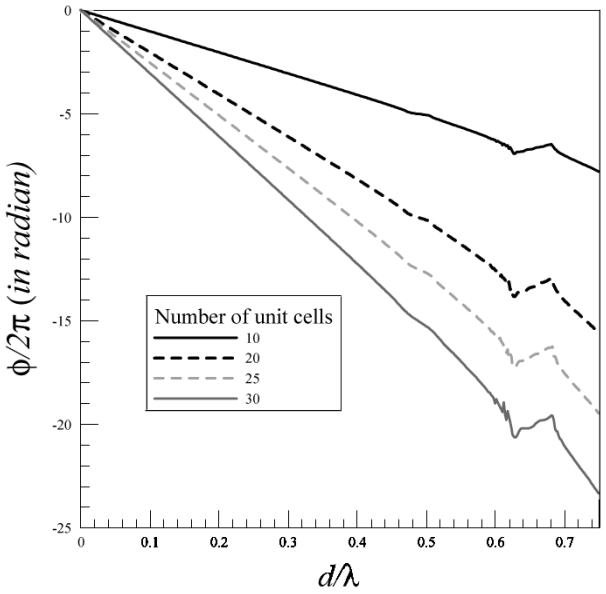

Fig. 8. Distribution of unwrapped phase versus normalized frequency for various lengths of corrugated waveguide.

Fig. 8 shows the variation of the phase angle, normalized to 2π, against the normalized frequency for various lengths (numbers of unit cells) of the CPPWG. The delay phase angle (absolute value) was found to increase with length. Therefore, the phase constant should be positive ($\beta = -\Delta\phi/\Delta L$). Hence, the wave in the slanted stopband region exhibits a positive phase velocity and a negative group velocity.

V. Conclusion

This investigation presented the NGV property and anomalous transmission of a wave propagating in a corrugated parallel-plate waveguide (CPPWG). Two schemes, scattering analysis of a finite length CPPWG and dispersion relation of an infinite CPPWG, were utilized to verify these anomalous phenomena. The NGV was found to occur in the slanted stop band, owing to the interaction between the space harmonic of the higher-order and the fundamental parallel-plate waveguide modes. Additionally, the anomalous transmittance resulting from the excitation of the higher-order mode in the stopband region was also observed and interpreted.

Acknowledgment

The authors wish express his gratitude to Professor S. T. Peng, National Chiao Tung University, Hsinchu, Taiwan, R.O.C., and Professors T. Tamir and Ming Liang, Polytechnic University, New York, for their mentoring in the area of periodic structure and for their encouragement in this research.

References

[1] C. G. B. Garrett and D. E. McCumber, "Propagation of a gaussian light pulse through an anomalous dispersion medium," *Phys. Rev. A, Gen. Phys.*, vol. 1, no. 12, pp. 305–313, Feb. 1970.

[2] S. Chu and S. Wong, "Linear pulse-propagation in an absorbing medium," *Phys. Rev. Lett.*, vol. 48, pp. 738–741, 1982.

[3] R. Y. Chiao and A. M. Steinberg, "Tunneling times and superluminality," *Progress in Opt.*, vol. 37, pp. 345–405, 1997.

[4] E. L. Bolda, R. Y. Chiao, and J. C. Garrison, "Two theorems for the group velocity in dispersive media," *Phys. Rev. A, Gen. Phys.*, vol. 48, pp. 3890–3894, Nov. 1993.

[5] M. Mojahedi, K. J. Malloy, G. V. Eleftheriades, J. Woodley, and R. Y. Chiao, "Abnormal wave propagation in passive media," *IEEE J. Select. Topics Quantum Electron.*, vol. 9, pp. 30–39, Jan./Feb. 2003.

[6] O. F. Siddiqui, M. Mojahedi, and G. V. Eleftheriades, "Periodically loaded transmission line with effective negative refractive index and negative group delay," *IEEE Trans. Antennas Propag.*, vol. 51, no. 10, pp. 2619–2625, Jun. 2003.
[7] F. Elek and G. V. Eleftheriades, "Dispersion analysis of Sievenpiper's shielded structure using multi-conductor transmission-line theory," *IEEE Microwave Wireless Components Lett.*, vol. 14, no. 9, pp. 434–436, Sep. 2004.
[8] S. Ramo, J. R. Whinnery, and T. Van Duzer, *Field and Waves in Communication Electronics*, 3rd ed. New York: Wile, 1994, ch. 9, p. 483.
[9] W. Rotman, "A study of single surface corrugated guides," in *Proc. IRE*, vol. 39, Aug. 1951, pp. 952–959.
[10] R. S. Elliott, "On the theory of corrugated plane surfaces.," *IRE Trans. Antennas Propag.*, vol. 2, pp. 71–81, Apr. 1954.
[11] L. O. Goldstone and A. A. Oliner, "A note on surface waves along corrugated structures," *IRE Trans. Antennas Propag.*, vol. 7, pp. 274–276, Jul. 1959.
[12] R. E. Collin, *Field Theory of Guided Waves*, 2nd ed. New York: IEEE Press, 1991.
[13] R. S. Elliott, *Antenna Theory and Design*. New York: IEEE Press, 2003. Revised Edition.
[14] R. C. Hall, R. Mittra, and K. M. Mitzner, "Analysis of multilayered periodic structures using generalized scattering matrix theory," *IEEE Trans. Antennas Propag.*, vol. 36, no. 4, pp. 511–517, Apr. 1988.
[15] N. A. Nicorovici and R. C. McPhedran, "Lattice sums of off-axis electromagnetic scattering by gratings," *Phys. Review E*, vol. 50, pp. 3143–3160, 1994.
[16] R.Bing Hwang, "Relations between the reflectance and band structure of 2-D metallodielectric electromagnetic crystals," *IEEE Trans. Antennas Propag.*, vol. 52, no. 6, pp. 1454–1464, Jun. 2004.
[17] S.Tsuen Peng, "Guided waves on 2D periodic structures and their relation to planar photonic band gap structures," in *Proc. Invited Speech, Asia-Pacific Microwave Conf.*, Yokohama, Japan, 1998.

A Note on Mass Lumping in the Finite Element Time Domain Method

Robert Lee

***Abstract*—Mass lumping has been used to produce explicit time integration schemes for the finite element time domain method. In this paper, we show that a specific choice in the lumping procedure can produce a scheme that is equivalent to the finite difference time domain method. If lumping is done in the time integration process, one can show that it can be equivalent to the Newmark-beta method.**

***Index Terms*—Finite element methods, finite-difference time-domain (FDTD) methods.**

I. Introduction

The concept of mass lumping has been around for a long time [1]. In electromagnetic applications it has been used as far back as 1990 [2]. Mass lumping is used in finite element time domain (FETD) methods to make the time integration scheme explicit through the diagonalization of the mass matrix. However, for tetrahedral edge elements, it is well known that a singular matrix may result [3]. Approaches to overcome this problem have been proposed [4], but in general, the use of mass lumping has been restricted to hexahedral (quadrilaterals in 2-D) elements.

Manuscript received July 26, 2005; revised October 14, 2005. This work was supported in part by the AFOSR under Grant FA9550-04-1-0359.

The author is with the ElectroScience Laboratory, Department of Electrical and Computer Engineering, The Ohio State University, Columbus, OH 43212 USA (e-mail: Lee.146@osu.edu).

Digital Object Identifier 10.1109/TAP.2005.863159

Recently, mass lumping concepts have been used to hybridize the FETD method with the finite-difference time-domain (FDTD) method. [5]. More importantly, the FDTD method can be shown to be equivalent to the FETD method on block elements with the proper choice of lumping. Thus, many advances that are made possible by the mathematical rigor inherent in finite element formulations can be adapted directly to the FDTD method. One such demonstration of this approach is shown in [6] where a stable sub-gridding scheme for FDTD is developed with the aid of FETD concepts.

In this paper, mass lumping is presented to show how the FETD and FDTD methods are related for the cases where the lowest order vector finite element basis functions (or edge elements) are used for the block element in 3-D and the rectangular element in 2-D. Finally, we consider the use of finite elements to discretize the time variable. This approach to handling time integration is seldom considered. Instead, one usually uses finite difference concepts such as the Newmark-beta method [7] to generate the time recurrence. One can show that these two approaches can be equivalent if lumping is applied to the time integral.

II. Lumping in Space

Let us consider the semi-discrete finite element approximation for the wave equation

$$\mathbf{T}\frac{d^2\{E\}}{dt^2} + \mathbf{S}\{E\} = 0. \tag{1}$$

The vector $\{E\} = [E_1, E_2, \ldots, E_j, \ldots, E_J]^T$ represents the time dependent unknowns associated with the vector finite element basis functions $\vec{w}_j$ for the block or rectangular elements [8]. The terms in the mass matrix $\mathbf{T}$ and the stiffness matrix $\mathbf{S}$ are given by

$$\mathbf{T}_{ij} = \frac{\varepsilon_r}{c^2}\int \vec{w}_i \bullet \vec{w}_j \, dv \tag{2}$$

$$\mathbf{S}_{ij} = \frac{1}{\mu_r}\int (\nabla \times \vec{w}_i) \bullet (\nabla \times \vec{w}_j) dv. \tag{3}$$

To obtain a fully discrete equation, a common approach is to use the Newmark-beta method for time integration. The following recurrence equation is obtained:

$$\begin{aligned}[\mathbf{T} + (\Delta t)^2 \Theta \mathbf{S}]\{E\}^{n+1} &= [2\mathbf{T} + (\Delta t)^2(2\Theta - 1)\mathbf{S}]\{E\}^n \\ &\quad - [\mathbf{T} + (\Delta t)^2\Theta\mathbf{S}]\{E\}^{n-1}.\end{aligned} \tag{4}$$

To obtain an explicit scheme, the matrix on the left hand side of (4) must be diagonalized. The typical approach is to choose $\Theta = 0$ and then to apply lumping to the mass matrix. The concept of mass lumping can be viewed as finding an approximate integration scheme for (2) that diagonalizes the mass matrix without compromising the overall accuracy of the numerical solution. For hyperbolic problems, the required accuracy is well known [9]. For basis functions of order k, the integration must be accurate to order $2k - 2$. Thus for linear basis functions $(k = 1)$, the trapezoidal rule is a valid choice for integration. Let us consider the 1-D case where the integral in (2) is just a single integral and the basis functions are the typical rooftop functions. Then the evaluation of $\mathbf{T}_{ij}$ over a single element of length h is

$$\mathbf{T}_{ij} = \frac{\varepsilon_r}{c^2}\begin{cases} h/3 & i = j \\ h/6 & i \neq j. \end{cases} \tag{5}$$

If the trapezoidal integration is used, then the integral over a single element is given by

$$\int_{x_1}^{x_2} f(x)dx = \frac{h}{2}(f(x_1) + f(x_2)). \tag{6}$$